EUROPEAN ORGANISATION FOR NUCLEAR RESEARCH

CERN-PPE/93-153
August 9th, 1993

Measurement of $b\bar{b}$ Correlations at the CERN $p\bar{p}$ Collider

UA1 Collaboration, CERN, Geneva, Switzerland

Aachen[1] - Amsterdam (NIKHEF)[2] - Birmingham[3] - CERN[4] - Helsinki[5] - Kiel[6] - Imperial College, London[7] - Queen Mary and Westfield College, London[8] - MIT[9] - Rutherford Appleton Lab[10] - Saclay[11] - UCLA[12] - Vienna[13]

C. Albajar[4], K. Ankoviak[12], S. Bartha[6], A. Bezaguet[4], A. Böhrer[1], K. Bos[2], C. Buchanan[12], B. Buschbeck[13], H. Castilla-Valdez[12], P. Cennini[4], S. Cittolin[4], E. Clayton[7], D. Cline[12], J.A. Caughlan[10], D. Dau[6], C. Daum[2], M. Della Negra[4], M. Demoulin[4], D. Denegri[11], H. Dibon[13], J. Dorenbosch[2], J.D. Dowell[3], K. Eggert[4], E. Eisenhandler[8], N. Ellis[3,4], H. Evans[12], H. Faissner[1], I.F. Fensome[3], L. Fortson[12], J. Garvey[3], A. Geiser[1,4], A. Givernaud[4], A. Gonidec[4], B. Gonzalez[12*], J. Gronberg[12], D.J. Holthuizen[2], W. Jank[4], G. Jorat[4], P.I.P. Kalmus[8], V. Karimäki[5], I. Kenyon[3], R. Kinnunen[5], M. Krammer[13], S. Lammel[1], M.P.J. Landon[8], Y. Lemoigne[11], S. Levegrün[6], P. Lipa[13], C. Markou[7], M. Markytan[13], G. Maurin[4], S. McMahon[7], J.P. Merlo[11], T. Meyer[4], T. Moers[1], M. Mohammadi[12], A. Morsch[6,4], A. Moulin[1], A. Norton[4], S. Otwinowski[12], G. Pancheri[9], E. Pietarinen[5], M. Pimiä[5], A. Placci[4], J.P. Porte[4], R. Priem[1], R. Prosi[6], E. Radermacher[4], M. Rauschkolb[6],H. Reithler[1], J.P. Revol[9,4], D. Robinson[8], C. Rubbia[4], D. Samyn[4], D. Schinzel[4], R. Schleichert[1], M. Schröder[2], C. Seez[7], T.P. Shah[10], P. Sphicas[9], K. Sumorok[9], F. Szoncso[13], C.H. Tan[9], A. Taurok[13], L. Taylor[7], S. Tether[9], H. Teykal[1], G. Thompson[8], H. Tuchscherer[1], J. Tuominiemi[5], W. van de Guchte[2], A. van Dijk[2], M. Vargas[12], T.S. Virdee[7], W. von Schlippe[8], V. Vuillemin[4], K. Wacker[1], H. Wagner[1], G. Walzel[13], C.-E. Wulz[13], and P. Zotto[4]

(submitted to Z. Phys. C)

(* deceased)

Abstract. We report on measurements of correlated $b\bar{b}$ production in $p\bar{p}$ collisions at $\sqrt{s} =$ 630 GeV, using dimuon data to tag both the b and $\bar{b}$ quarks. Starting from an inclusive dimuon sample we obtain improved cross-sections for single inclusive beauty production and confirm our earlier results on B^0-$\bar{B}^0$ mixing. From a study of $b\bar{b}$ correlations we derive explicit cross-sections for semi-differential $b\bar{b}$ production. We compare the measured cross-sections and correlations to $O(\alpha_s^3)$ QCD predictions and find good quantitative agreement. From the measured angular distributions we establish a sizeable contribution from higher order QCD processes with a significance of about seven standard deviations. A large nonperturbative contribution to these higher order corrections is excluded.

1 Introduction

The CERN Sp$\bar{p}$S collider is a copious source of $b\bar{b}$ pairs. The measured total $b\bar{b}$ cross-section of 20 μb [1] corresponds to the production of 10^8 $b\bar{b}$ events within the UA1 detector during the 1988 and 1989 runs upon which this study is based. A representative fraction of these b quarks is detected in UA1 through their semileptonic decays, yielding high p_T[1] nonisolated[2] muons.

High p_T muons can however also arise from other processes such as charm production, Drell-Yan production of lepton pairs, decays of heavy vector mesons (Υ,J/ψ) etc., which are all interesting in their own right. We will therefore start with an inclusive analysis of all possible processes giving rise to dimuon events and show that the data sample can be well understood in terms of these processes. A detailed analysis of the subsample of isolated muon events, focused on Υ and Drell-Yan production, is the subject of a separate paper [2]. Here we will concentrate on the predominantly nonisolated contribution from $b\bar{b}$ (and $c\bar{c}$) events.

In previous UA1 analyses [1, 3], cross-sections for single inclusive b quark production were obtained from four different processes:

- single muon (+ jet) production via semileptonic decays: $p\bar{p} \rightarrow b \rightarrow \mu$
- J/ψ production from b decays: $p\bar{p} \rightarrow b \rightarrow J/\psi \rightarrow \mu^+\mu^-$
- b chain decays: $p\bar{p} \rightarrow b \rightarrow c + \mu$, $c \rightarrow \mu$
- semileptonic decays of both b quarks: $p\bar{p} \rightarrow b\bar{b}$, $b \rightarrow \mu$, $\bar{b} \rightarrow \mu$

where 'b' symbolizes either of the two quarks from a $b\bar{b}$ pair, '$b \rightarrow \mu$' stands generically for both first or second generation semileptonic decay ($b \rightarrow \mu X$ or $b \rightarrow c \rightarrow \mu X$) and other final state particles like neutrinos and hadrons are omitted for simplicity.

Only the last of these four processes allows the direct measurement of $b\bar{b}$ correlations. Charge correlations between the two resulting muons have been used earlier to measure B^0-$\bar{B}^0$ mixing [4, 5]. In this analysis, the scope is extended towards a quantitative study of 4-momentum correlations (invariant mass, angular distributions). Early qualitative results on such correlations from the 1983-85 data [6, 7] are reviewed in [8].

[1] transverse momentum with respect to the beam axis

[2] accompanied by hadrons from fragmentation and decay

There is a twofold motivation for an in-depth study of $b\bar{b}$-correlations:

- The topology of the produced $b\bar{b}$ pair permits discrimination between different QCD production mechanisms. Hence the QCD-predicted production rates for these processes can be tested.
- A correct description of $b\bar{b}$ correlations is essential for the derivation of single inclusive b quark cross-sections from events where both b quarks are explicitly detected.

We use the measured muon angular correlations to obtain cross-sections for $b\bar{b}$ production as a function of the $b\bar{b}$ angular separation. A quantitative comparison of these semi-differential cross-sections with QCD predictions has become possible following a recent fully differential calculation of $b\bar{b}$ production to order α_s^3 by Mangano, Nason, and Ridolfi [9]. Furthermore, the explicit measurement of the $b\bar{b}$ correlations is used to reduce the error on the single b quark acceptance from this source and to yield improved measurements of the single inclusive b quark cross-section and B^0-$\bar{B}^0$ mixing from dimuon events. A measurement of α_s is derived from the measured semi-inclusive cross-sections in a separate paper [10].

2 The UA1 detector

A detailed description of the UA1 detector can be found elsewhere [11]. In brief, as particles leave the interaction vertex, they first encounter a large volume drift chamber, the central detector (CD). Here, the momenta of charged particles are measured in a 0.7 T dipole magnetic field, with a typical accuracy on $\Delta p/p$ of $0.01 \times p$ (GeV/c) for a 1 m long track. After an air gap of 0.5 - 1 m, the particles next encounter the (hadronic) calorimeter and at least 60 cm of additional iron shielding. Together, the calorimeter and the shielding wall correspond to more than 8 interaction lengths of material, which almost completely absorb strongly interacting particles. The iron shielding is partially instrumented with limited streamer tubes measuring the position of minimum ionizing particles. Finally, muons are detected in the outer muon chambers, which cover about 75% of the solid angle in the pseudorapidity range $|\eta| < 2.3$. Muon trigger processors require tracks in the muon chambers which point back to the interaction region. These processors permit triggering with $|\eta| < 1.5$ for single high p_T muons, and with $|\eta| < 2.3$ for muon pairs.

3 The data sample

The analysis presented here is based on data collected with the UA1 detector during runs at the CERN $p\bar{p}$ collider from 1988 to 1989 with a total integrated luminosity of 4.7 pb^{-1}. Muons are identified as high p_T tracks in the CD, which when extrapolated through the iron shielding have corresponding tracks in the muon chambers. Dimuon events are selected requiring both tracks to originate from the primary interaction vertex

and to have $p_T > p_{Tcut} = 3$ GeV/c. This yields a final inclusive dimuon sample of 3846 events [12].

For the 1984/85 data, the corresponding sample had been separated into high [6] and low [13] mass subsamples as suggested by the topological threshold at $m_{\mu\mu} = 2p_{Tcut}/c = 6$ GeV/c^2: For low masses $m_{\mu\mu}$, the requirement of large transverse momentum for each muon implies a sizeable transverse momentum of the dimuon system [13] and hence a nearly collinear muon pair configuration. For masses larger than 6 GeV/c^2, the anti-collinear muon configuration becomes allowed, resulting in a corresponding rise in the topological acceptance.

In this paper we drop this physically arbitrary separation and consider the inclusive sample up to[3] $m_{\mu\mu} = 35$ GeV/c^2. To separate muon pairs originating from the same or from different parent particles a cut at $m_{\mu\mu} = 4$ GeV/c^2 is applied for part of the analysis. Muon pairs originating from b chain or J/ψ decays or from light vector mesons will lie below this cut [13].

To separate e.g. the Drell-Yan and heavy flavour contributions we also classify the events according to the muon charge and isolation, i.e. the amount of hadronic activity surrounding the muon. For practical purposes[4], a cone of $\Delta R = \sqrt{\Delta\eta^2 + \Delta\phi^2} < 0.7$ in pseudorapidity-azimuth space around each muon direction is considered. The isolation definition is made dependent on the event topology. If the two muons are far apart ($\Delta R_{\mu\mu} > 1.4$) we define

$$I_i \equiv \sqrt{(\Sigma_i E_T/2)^2 + (\Sigma_i p_T)^2} \tag{1}$$

where $i = 1, 2$ designates the cones around muons 1 and 2, and $\Sigma_i E_T$ ($\Sigma_i p_T$) is the sum of the transverse energy (momentum) within each cone. We further define the combined variable

$$S \equiv I_1^2 + I_2^2 \tag{2}$$

and require $S < 8$ GeV^2 to classify the muon pair as being isolated.

However, if both muons originate from the same parent particle, the two muons are close together and their cones overlap ($\Delta R_{\mu\mu} < 1.4$). For this case we therefore define

$$I_{\mu\mu} \equiv \sqrt{(\Sigma_{\mu\mu} E_T/2)^2 + (\Sigma_{\mu\mu} p_T)^2} \tag{3}$$

where the cone is now taken around the *dimuon* momentum direction, and require $I_{\mu\mu} <$ 2.5 GeV *and* $I_1 < 2.5$ GeV *and* $I_2 < 2.5$ GeV for an isolated muon pair.

Excluding events with $m_{\mu\mu} > 35$ GeV/c^2 the event sample can be broken down into 1115 isolated unlike sign, 151 isolated like sign, 1782 nonisolated unlike sign, and 744 nonisolated like sign dimuon events. Note that the results obtained in this paper do not critically depend upon the details of the isolation definition.

[3]The Z^0 mass region, outside of the scope of this analysis, is treated in a separate paper [14].

[4]See ref. [17] for a motivation of the isolation variable definitions

4 Monte Carlo and background calculations

High statistics Monte Carlo simulations of all the processes producing prompt, high p_T muons have been made using ISAJET [15]. In particular, these include the simulation of heavy quark ($b\bar{b}$,$c\bar{c}$) production for 3 classes of subprocesses (fig. 1) called flavour creation, flavour excitation (initial state gluon splitting) and final state gluon splitting, including possible additional gluon radiation through the parton shower approach. We will also refer to the flavour creation process as 'ISAJET lowest order' process and to the flavour excitation and gluon splitting processes as 'ISAJET higher order' processes.

As outlined in ref. [16], these processes give a phenomenologically acceptable but theoretically incomplete description of QCD heavy flavour processes. To improve this phenomenological description we leave the relative normalization of these three subprocesses free to be determined from the data by the fit described in section 5.

For $b\bar{b}$ production we have also implemented a quasi-$O(\alpha_s^3)$ QCD Monte Carlo program [12] by effectively replacing the ISAJET parton generator by the fully differential QCD calculation of ref. [9] while keeping the procedures for fragmentation, decay, and treatment of the underlying event. This effective $O(\alpha_s^3)$ matrix element Monte Carlo is used for all acceptance calculations in this paper, therefore avoiding the uncertainties related to the ISAJET parton shower approach. It unfortunately does not allow a breakdown according to the subprocesses discussed above, and can therefore not replace ISAJET for this purpose.

All Monte Carlo events are subjected to a detailed simulation of the detector response, followed by the same reconstruction and selection procedure as for the data.

About 25% of the data are expected to originate from non-prompt muon backgrounds. The dominant background from kaon and pion decays in flight is obtained from a calculation based on real data events. As described in ref. [5] hadrons in measured events are assumed to decay, simulating the appropriate detector response. The small ($\lesssim 2\%$) backgrounds from other sources (e.g. punchthrough, cosmic ray muons) are also reliably estimated [12].

5 Fit of the dimuon mass and angular distributions

In this analysis, we use the strong correlation between the properties of the parent b quarks and the resulting semileptonic decay muons to measure $b\bar{b}$ correlations. To be able to extract the corresponding heavy flavour contribution from the data, the background due to non-heavy flavour sources must be well understood. The study of dimuon correlations (mass and angular distributions) is particularly well suited to achieve both of these goals due to its high discrimination power between the various event topologies. Fig. 2 shows the mass distributions for unlike sign dimuon events. Mass peaks at vector meson resonances (Υ, J/ψ, ρ etc.) are clearly visible. Angular distributions for nonisolated events are shown in fig. 3. The peak at $\Delta\phi = 180°$ indicates the dominance of the back-to-back configuration for heavy flavour events in the sample. This is consistent with

the expectation that the sizeable higher order QCD contribution (section 8) is partially suppressed due to a lower acceptance.

We perform a *simultaneous inclusive fit* to these distributions for the 1988/89 dimuon data, taking into account their correlations[5]. The basic principle of the fit is to use the *shapes* of the various distributions obtained from the Monte Carlo or background calculations[6], and to fit their respective normalization to the data.

A detailed technical description of the fitting procedure and the corresponding results can be found in ref. [12]. In short, the distributions fitted simultaneously are:

- the dimuon mass distributions in the range $2m_\mu < m_{\mu\mu} < 35$ GeV/c^2 for like and unlike sign, isolated and nonisolated muon pairs (fig. 2).
- $\Delta\phi(\mu\mu)$ for nonisolated events with $m_{\mu\mu} > 4$ GeV/c^2, independent of the muon charge, where $\Delta\phi$ is the azimuthal angle difference between the two muons (fig. 3).
- $\Delta R(\mu\mu)$ for these same events, with the additional requirement $\Delta\phi(\mu\mu) < 120°$ ($\Delta R = \sqrt{\Delta\eta^2 + \Delta\phi^2}$) (fig. 3).

The $\Delta\phi$ cut for the ΔR distribution is introduced because the intended interpretation of ΔR as an approximate angle in space is no longer meaningful for large $\Delta\phi$ values.

The parameters fitted without constraint are:

- the normalization of the total heavy flavour ($b\bar{b}+c\bar{c}$) and b chain decay contributions
- the fractions of higher order contributions (flavour excitation and gluon splitting) to $b\bar{b} + c\bar{c}$
- the B^0-$\bar{B}^0$ mixing parameter χ (see section 6)
- the normalization of the Drell-Yan, Υ, J/ψ, $\psi\prime$, and light meson contributions.

Other parameters are fitted with constraints imposed from external measurements:

- the $c\bar{c}/(b\bar{b}+c\bar{c})$ fraction and the fraction of $b\bar{b}$ 2nd generation decays are constrained to values extrapolated from independent fits of p_T^{rel} distributions [1, 5], where p_T^{rel} is the p_T of the muon relative to the jet axis,
- the K/π decay and other background contributions are fitted with Gaussian constraints obtained from the absolute predictions of the decay background calculations, and from the extrapolation of the p_T^{rel} fit [5],
- all isolated event fractions are fluctuated within the errors obtained from detailed isolation studies [17].

[5] While the mass distributions are completely independent of each other, there is a considerable overlap and also some correlation between the mass and angular distributions. The distortion of the fit results due to these correlations were however found to be small and are taken into account [12].

[6] Gaussian shapes were assumed for the various vector meson decays

This choice of the parameters and an appropriate binning ($\gtrsim 10$ events per bin) yields a χ^2-fit which is both quickly converging and stable against variations of the starting values within the physically sensible ranges. The χ^2 is 234 for 214 degrees of freedom.

Table 1: *Fitted contributions to the inclusive dimuon sample from various processes obtained from the overall dimuon mass and angle fit for $m_{\mu\mu} < 35$ GeV/c^2. In addition to the statistical error, the quoted errors also include the systematic errors on the isolation definition and background subtraction.*

process	events
Drell-Yan	486 ± 54
$\Upsilon + \Upsilon' + \Upsilon''$	208 ± 35
$J/\psi + \psi\prime$	363 ± 22
$\rho + \omega + \phi + \eta + \eta\prime$	234 ± 34
b chain decays	102 ± 26
$b\bar{b} + c\bar{c}$ (muons from different quarks)	1286 ± 89
background	955 ± 84

The qualitative results of this *overall mass and angle fit* are shown in figs. 2 and 3 and a summary of some inclusive results is listed in table 1. All fitted contributions are in good agreement with the results from earlier measurements [6, 13] and with the expectations from the Monte Carlo calculations.

The analysis of J/ψ production has already been published earlier [18], including the first evidence for the decay $\Lambda_b \rightarrow J/\psi\Lambda$ [19]. The analysis of the predominantly isolated Υ and Drell-Yan contributions is the subject of a separate paper [2]. Noting that the background from non-heavy-flavour sources is well understood, we will now focus on the mainly nonisolated contribution from heavy flavour semileptonic decays.

6 Heavy flavour production and B^0-$\bar{B}^0$ mixing

The subset of results of the overall mass and angle fit relevant for heavy flavour production will now be considered in more detail.

While the b chain decay contribution is restricted almost exclusively to the nonisolated unlike sign sample (fig. 2) where it is easily identified in the mass region around 2 GeV/c^2, the $b\bar{b}$ and $c\bar{c}$ contributions with muons from different quarks spread out over all distributions, including the like sign events in the $b\bar{b}$ case. Particularly $b\bar{b}$-enriched subsamples can be found in the distributions for nonisolated high mass events.

A further study of heavy flavour production requires the separation of $b\bar{b}$ and $c\bar{c}$ events and the separation of 1st and 2nd generation $b\bar{b}$ decays[7]. Both of these can only poorly be achieved from the mass and angle fit alone. On the other hand, the p_T^{rel} variable[8] introduced in refs. [1, 5] yields a good handle for such a separation.

Since the p_T^{rel} distributions are complementary to the dimuon mass and angular distributions we have effectively combined the two fits by imposing the results from ref. [5] on the $c\bar{c}$, 2nd generation $b\bar{b}$, and background fractions as external constraints to the relevant subsamples of the overall mass and angle fit [12]. The corresponding results are listed in table 2.

Table 2: *Fitted number of events for each heavy flavour process in the overall mass and angle fit, separated according to dimuon charge, mass and isolation. Note that the fraction of like sign and unlike sign events for each of the 1st and 2nd generation $b\bar{b}$ subprocesses is a consequence of B^0-$\bar{B}^0$ mixing only and does not depend on mass or isolation cuts. The charge fractions quoted for all events are therefore also valid for each mass and isolation subsample. The $c\bar{c}$ and b chain decay contributions only yield unlike sign dimuons.*

process	all	like sign	unlike sign	$m_{\mu\mu} < 6$ GeV/c^2		$m_{\mu\mu} > 6$ GeV/c^2	
				isol	not isol	isol	not isol
1st generation $b\bar{b}$	933.5	247.1	686.4	12.9	49.6	209.0	662.0
2nd generation $b\bar{b}$	219.0	161.0	58.0	1.7	11.7	18.3	187.3
$c\bar{c}$	132.6	–	132.6	0.6	7.4	6.2	118.4
b chain decays	101.6	–	101.6	17.4	84.2	–	–

The $c\bar{c}$ contribution is suppressed with respect to $b\bar{b}$ mainly due to the softer fragmentation and correspondingly softer decay muons, while 2nd generation decays are suppressed because the muon picks up a smaller fraction of the b quark momentum compared to a muon from a 1st generation decay. The fraction of muons produced with the 'wrong' charge due to B^0-$\bar{B}^0$ mixing is described by the parameter $\chi = f_d\chi_d + f_s\chi_s$, where χ_d and χ_s are the mixing parameters in the B_d^0 and B_s^0 sectors, and $f_{d(s)}$ are the probabilities for

[7]The term '1st generation $b\bar{b}$' is used for events in which both b quarks decay semileptonically in 1st generation, and '2nd generation $b\bar{b}$' denotes events in which one of the b's decays in 1st and the other in 2nd generation. The small fraction of events in which both quarks decay in 2nd generation is technically included into the '1st generation' subsample.

[8]p_T of the muon with respect to the axis of the accompanying hadronic jet.

the fragmentation of a $\bar{b}$ quark into $B^0_{d(s)}$ mesons, with slight corrections due to possibly different semileptonic branching ratios. The formulae for the measurement of χ from the observed event samples are described in ref. [5].

The evaluation of the fitted numbers of like sign and unlike sign events in the overall mass and angle fit in terms of these formulae yields a value for the B^0-$\bar{B}^0$ mixing parameter

$$\chi = 0.157 \pm 0.020_{stat} \pm 0.032_{sys} \quad (4)$$

which is consistent with the result of our earlier dedicated analysis based mainly on the p_T^{rel} distributions, $\chi = 0.148 \pm 0.029_{stat} \pm 0.017_{sys}$ [5]. The systematic error on χ is dominated here by the residual contribution from Upsilon and Drell-Yan events to the nonisolated subsample, which had been removed in the earlier analysis by demanding that the muons be embedded in a loosely defined jet [5]. Since the two results are strongly correlated (overlapping event samples, correlated systematics), a combination of the two measurements would not yield a significantly improved result [12], and is therefore omitted.

7 Cross-sections for inclusive beauty production

To derive cross-sections for single inclusive beauty production as a function of p_{Tb}, the inclusive dimuon sample is subdivided into four p_T bins from 3 to 20 GeV/c (table 3). For events with $m_{\mu\mu} > 4$ GeV/c^2, the p_T cuts refer to the *highest p_T muon* per event only. No restrictions are applied to the lower p_T muon in addition to the default requirement of $p_{T\mu} > 3$ GeV/c. For $b\bar{b}$ events, this is roughly equivalent to a cut on the p_T of the higher p_T b quark of each pair. For events with $m_{\mu\mu} < 4$ GeV/c^2 the cut is applied to the *p_T of the dimuon system* instead, resulting in an effective cut on the p_T of the single parent b quark for b chain decays.

The relevant results of the overall mass and angle fit applied separately to the data in these four p_T ranges are listed in table 3. Note that in the $p_{T\mu\mu}$ range 3-5 GeV/c there is no acceptance for b chain decays due to the p_T cut on the individual muons, while in the range 5-7 GeV/c the acceptance is too small to yield a significant measurement.

Correcting for acceptance, we obtain cross-sections for dimuon production from b chain and $b\bar{b}$ semileptonic decays (table 4). Using the method outlined in [1], we can translate these into cross-sections for inclusive single b quark and B hadron production. Here, 'B hadron' stands for the most direct parent hadron containing a b quark (excluding $\bar{b}$), while 'b quark' denotes the quark at the origin of the b quark jet before fragmentation and radiation of collinear gluons within $\Delta R < 1$. The resulting cross-sections for $|y| < 1.5$ are summarized in table 5. Although the dimuon measurements extend up to $|y| < 2.3$, the rapidity range $|y| < 1.5$ has been chosen for compatibility with earlier measurements [1]. The quoted errors result from the following uncertainties:

- The error on the muon level cross-sections, including the statistical error and the errors on acceptance (11%) integrated luminosity (8 %), and background subtraction.

Table 3: *Fitted number of heavy flavour events for each p_T bin in the overall mass and angle fit, where $p_T \equiv p_{T\mu}^{high}$ for $m_{\mu\mu} > 4$ GeV/c^2 and $p_T \equiv p_{T\mu\mu}$ for $m_{\mu\mu} < 4$ GeV/c^2 (see text). The results for other processes can be found in [12].*

p_T range:	3-5 GeV/c	5-7 GeV/c	7-10 GeV/c	10-20 GeV/c
process:				
$b\bar{b}$	608 ± 58	377 ± 32	140 ± 19	39 ± 9
$c\bar{c}$	82 ± 23	31 ± 10	9 ± 3	2 ± 1
b chain decays	–	0 ± 10	48 ± 19	43 ± 12

Table 4: *Cross-sections for dimuon production from semileptonic beauty decays in $p\bar{p}$ collisions at $\sqrt{s} = 630$ GeV. Both muons are required to have $p_T > 3$ GeV/c and $|\eta| < 1.5$. A mass cut 6 GeV/$c^2 < m_{\mu\mu} < 35$ GeV/c^2 is applied for muons from different quarks, and additional p_T cuts are applied either to the higher p_T muon ($p_T^{\mu_1}$) or to the dimuon system ($p_T^{\mu\mu}$).*

process	$\sigma(p\bar{p} \to b(\bar{b}) \to \mu\mu X)$ [pb]
dimuons from diff. b's	
$p_T^{\mu_1} = 3 - 5$ GeV/c	879 ± 146
$p_T^{\mu_1} = 5 - 7$ GeV/c	551 ± 88
$p_T^{\mu_1} = 7 - 10$ GeV/c	190 ± 36
$p_T^{\mu_1} = 10 - 20$ GeV/c	58 ± 15
b chain decays	
$p_T^{\mu\mu} = 7 - 10$ GeV/c	93 ± 39
$p_T^{\mu\mu} = 10 - 20$ GeV/c	89 ± 28

Table 5: *The inclusive single b quark (Q=-1/3) and B hadron (including b-baryon) cross-sections for* $|y_b| < 1.5$ *and* $p_{Tb} > p_{Tb}^{min}$ *in* $p\bar{p}$ *collisions at* $\sqrt{s} = 630$ *GeV. For comparison, the superseded results of ref. [1] are quoted in parenthesis. The errors for the updated measurements are subdivided into a* p_T*-dependent (1st error) and a common* p_T*-independent part (2nd error).*

process	$p_T^{min}(b)$ [GeV/c]	$\sigma(p_{Tb} > p_T^{min})$ [nb]	$p_T^{min}(B)$ [GeV/c]	$\sigma(p_{TB} > p_T^{min})$ [nb]
dimuons from diff. b's				
($p_T^{\mu_1} > 3$ GeV/c [1])	(6)	(2660 ± 1330)	(5.5)	(2390 ± 1150)
$p_T^{\mu_1} = 3 - 5$ GeV/c	6	$2310 \pm 250 \pm 640$	5	$2570 \pm 280 \pm 640$
$p_T^{\mu_1} = 5 - 7$ GeV/c	8	$1300 \pm 110 \pm 360$	7	$1360 \pm 110 \pm 340$
$p_T^{\mu_1} = 7 - 10$ GeV/c	11	$385 \pm 54 \pm 106$	10	$315 \pm 44 \pm 79$
$p_T^{\mu_1} = 10 - 20$ GeV/c	15	$109 \pm 34 \pm 31$	13	$103 \pm 32 \pm 26$
b chain decays				
($p_T^{\mu\mu} > 6$ GeV/c [1])	(10)	(390 ± 170)	(9)	(340 ± 145)
$p_T^{\mu\mu} = 7 - 10$ GeV/c	11	$220 \pm 90 \pm 70$	10	$180 \pm 70 \pm 50$
$p_T^{\mu\mu} = 10 - 20$ GeV/c	15	$118 \pm 35 \pm 34$	13	$111 \pm 33 \pm 31$

- The uncertainty on the branching fractions and decay kinematics for 1st generation semileptonic decay (10%), 2nd generation semileptonic decay (18%), and the choice of the fragmentation function parametrization (6% per b quark). The corresponding values and errors have been obtained from e^+e^- data as described in [1].

- The shape of $d\sigma/dp_T^b$ used for the integration, and the shape of $d^2\sigma/dp_T^{b_1}dp_T^{b_2}$ used for the acceptance calculation. For the earlier measurements [1] which relied on the shapes given by the default ISAJET Monte Carlo program we included a 20% error per detected b quark. For the dimuon measurements of this analysis, which use the double differential shape predicted by the $O(\alpha_s^3)$ QCD calculation [9], this error is reduced from 20% to 10% for b chain decays, and from 40% to 6% for muonic decays of both b's. For the latter case, acceptance calculations were performed using both the ISAJET and $O(\alpha_s^3)$ double differential distributions with various assumptions, constrained to be compatible with the measured angular distributions (section 8). The maximum spread of the derived cross-sections was found to be $\pm 6\%$ [12].

Fig. 4 shows a comparison of these cross-sections with the $O(\alpha_s^3)$ QCD predictions of

Nason et al. [20]. The data points from single muon and J/ψ production from ref. [1] have also been included. The uncertainties in the prediction are due to the value of the b quark mass, the value of the QCD parameter Λ, the choice of the normalization/factorization scale μ and the choice of the structure functions. Good agreement for both shape and normalization is observed over the whole measured p_{Tb}^{min} range.

The extrapolation of the cross-sections in the p_{Tb}^{min} interval 6-15 GeV/c towards p_{Tb}^{min} =0 using the QCD-predicted shape yields a total cross-section for single b quark production in the restricted rapidity range $|y_b| < 1.5$

$$\sigma_{tot}(p\bar{p} \rightarrow bX, |y_b| < 1.5) = 13.0 \pm 2.8_{norm.}\ ^{+6.9}_{-4.3\ shape}\ \mu b \tag{5}$$

The first error is the error for the normalization of the $O(\alpha_s^3)$ QCD shape to the data points, fully accounting for their respective correlations [12]. It thus includes the experimental errors and the errors on fragmentation and decay. An additional error of 6% for the b quark definition (treatment of collinear gluon radiation) is also included.

The second error is obtained from a variation of the shape of the $O(\alpha_s^3)$ prediction within the theoretical uncertainties. This includes an error of 16% due to the choice of Λ_{QCD} and the structure functions, and an error of 10% due to the variation of m_b and μ/μ_0 (for fixed μ_0) within the limits quoted in fig. 4. The largest error of $^{+50\%}_{-27\%}$ is due to the variation of the definition of the reference scale $\mu_0 = \sqrt{(k \times m_b)^2 + p_T^2}$ with $2/3 < k < 3/2$ ($0.44 < k^2 < 2.3$) where the upper limit k_{max} is derived from the measured shape of the cross-section [12], and k_{min} is taken to be $1/k_{max}$. The variation of k mainly affects the shape of the prediction near $p_T = 0$, and is almost negligible for $p_T \gg m_b$.

Extrapolating to all rapidities using the predicted QCD shape[9] we obtain the *total cross-section for $b\bar{b}$ pair production* at the CERN p$\bar{\text{p}}$ collider

$$\sigma_{tot}(p\bar{p} \rightarrow b\bar{b}X) = 19.7 \pm 4.3_{norm}\ ^{+10.4}_{-6.5\ shape}\ \mu b \tag{6}$$

This result, which now includes a full theoretical error analysis, is consistent with our previous result of $19 \pm 7_{exp.} \pm 9_{th.}$ μb [1]. It is also in good agreement with the absolute QCD predictions of 19^{+10}_{-8} μb for $m_b = 4.5$ GeV/c^2 and 12^{+7}_{-4} μb for $m_b = 5.0$ GeV/c^2 from Altarelli et al. [22] using the Nason et al. calculation [23].

8 Measurement of $b\bar{b}$ angular correlations.

In contrast to e.g. inclusive jet production, a large contribution from higher order processes is expected for b production at hadron colliders. This can be explained by the fact that the dominant lowest order QCD process $gg \rightarrow gg$ ($\sigma(gg \rightarrow gg)/\sigma(gg \rightarrow Q\bar{Q}) \sim 100$) does not contribute to heavy flavour production in leading order. At next-to-leading order

[9]The possibility of a large cross-section for diffractive forward heavy flavour production is neglected in this assumption. Small upper limits on such a contribution have however been placed from a dedicated study [21].

however, one of the initial or final state gluons can split into a $b\bar{b}$ pair. The suppression of this splitting by kinematics and the additional factor α_s compensates the enhancement of the primary cross-section, yielding a contribution which is comparable in size to the leading order contribution. We will now try to identify this contribution by studying $b\bar{b}$ angular correlations.

For the dynamic range considered in this analysis, there is a very strong correlation between the measured muon directions and the directions of the parent b quarks: $\sigma(\Delta\phi(\mu\mu) - \Delta\phi(b\bar{b})) \sim 12°$. After background subtraction, the measured muon angular distributions can therefore directly be translated into the corresponding distributions for b quarks.

8.1 Muon angular correlations: A comparison with ISAJET

The study of muon angular correlations is part of the overall mass and angle fit (section 5). Since the main purpose of the angular fits is the study of the topology of $b\bar{b}$ correlations, the nonisolation requirement is chosen to suppress the Drell-Yan and Υ contributions, while the mass cut, $m_{\mu\mu} > 4$ GeV/c^2, eliminates J/ψ events, b chain decays, and the decays of low mass mesons. The ISAJET Monte Carlo was used for a description of the different heavy flavour contributions. The contributions from flavour creation, flavour excitation, and gluon splitting (fig. 1) were fitted *separately* and *without constraint*. The corresponding fit results are listed in table 6.

Before attempting an interpretation of the results, it should be remembered that the 'ISAJET higher order' definition (section 3) has some inherent weaknesses:

- Due to internal thresholds, the 'higher order' predictions for $p_{Tb} < 10$ GeV/c are very unreliable and partially unphysical. For example, 'flavour excitation' processes can not be generated below a p_T of the hard scattering process of 9 GeV/c.
- No interference effects are taken into account.
- The 'flavour creation' contribution used to define the 'lowest order' shapes does contain a contribution from hard initial and final state gluon radiation, which should in principle be counted as higher order processes.

With these restrictions in mind, the results from table 6 can be interpreted as follows:

In the two last bins, corresponding to parent b quarks with $p_{Tb} \gtrsim 11$ GeV/c or higher, ISAJET is expected to yield fairly reliable predictions. Indeed all measured higher order fractions agree with the corresponding ISAJET predictions within the (partially large) errors. In contrast, in the bins containing a large fraction of low p_T b quarks (all, 3-5, and 5-7) the fraction of events with 'gluon splitting' topology found in the data is at least a factor 2 below the ISAJET expectation, thus indicating an overestimation of this contribution by ISAJET. It is interesting however that this is compensated by the expected underestimation of the 'flavour excitation' contribution, such that the predicted *total* higher order fraction is in fair agreement with the data.

Table 6: *Fitted higher order contributions for each p_T bin in the overall mass and angle fit for nonisolated $b\bar{b}$ events with $m_{\mu\mu} > 4$ GeV/c^2. The higher order ('high.ord.') and final state gluon splitting ('gl.spl.') definitions are taken from ISAJET (see text). The higher order fractions relative to the ISAJET prediction (scale factors) are also given. The values in parenthesis are 90% c.l. upper limits for results compatible with 0.*

$p_{T\mu}^{high}$ range [GeV/c]	p_{Tb} range [GeV/c]	$b\bar{b}$ nonisol. $m_{\mu\mu} > 4$GeV/c^2 [events]	'high.ord.' fraction [%]	'high.ord.' fraction /ISAJET	'gl.spl.' fract. [%]	'gl.spl.' fraction /ISAJET
all	$\gtrsim 6$	829 ± 58	26.2 ± 4.0	1.16 ± 0.18	(< 6)	(< 0.49)
3-5	$\gtrsim 6$	402 ± 37	24.6 ± 8.5	1.22 ± 0.42	(< 9)	(< 0.70)
5-7	$\gtrsim 8$	286 ± 23	31.2 ± 5.4	1.34 ± 0.23	(< 8)	(< 0.48)
7-10	$\gtrsim 11$	103 ± 12	35.2 ± 5.1	1.23 ± 0.18	9 ± 5	0.68 ± 0.38
10-20	$\gtrsim 15$	32 ± 6	21.3 ± 12.4	0.75 ± 0.44	17 ± 11	1.13 ± 0.75

We will now consider these results in more detail.

Fig. 5 shows the measured and fitted $\Delta\phi$ and ΔR distributions for nonisolated muon pairs with $m_{\mu\mu} > 4$ GeV/c for the $p_{T\mu}$ bin from 7-10 GeV/c. The applied mass cut eliminates the contributions from b chain and $b \rightarrow J/\psi$ decays, such that the remaining heavy flavour contribution is guaranteed to contain muons originating from the two different quarks of a heavy quark pair. The considerably smaller statistics with respect to fig. 3 is compensated here by a very small background contribution. From table 6 it can be seen that the presence of the higher order contribution is established with a significance of about seven standard deviations.

The higher order contributions, enriched by the cut $\Delta\phi < 120°$, can then be studied in more detail in the ΔR distribution. In contrast to the other contributions, the 'gluon splitting' contribution yields muon pairs which are clustered towards small ΔR values. This is easily understandable in terms of the (quasi-)collinear emission of the heavy quarks resulting from a virtual high transverse momentum gluon. Unfortunately, very small ΔR values are cut away by the mass cut of 4 GeV/c^2 which is needed to eliminate the b chain and J/ψ contributions, thus further limiting the already poor statistics.

From these differences, an indication for the presence of such final state gluon splitting processes is obtained with a significance of about two standard deviations (table 6). Since the gluon-gluon initial state is expected to dominate in the kinematic range considered here this can also be interpreted as an indication for the presence of the 3-gluon vertex

(fig. 1). The highest $p_{T\mu}$ bin (10-20 GeV/c) qualitatively confirms these conclusions within the limited statistics.

In summary, the default ISAJET prediction already gives a fair phenomenological description of the data. The use of this ISAJET prediction for the cross-section determination from high mass dimuons in ref. [1] is therefore justified in hindsight. This phenomenological agreement is further improved by a variation of the relative contributions from the various subprocesses, achieving a very good description of the data.

8.2 Cross-sections for semi-differential $b\bar{b}$ production

To compare the data directly to the recent fully differential $O(\alpha_s^3)$ QCD prediction [9] the measured muon angular distributions have to be converted into corresponding distributions for $b\bar{b}$ pairs. Furthermore, the cuts applied at the muon level must be translated into approximately equivalent cuts on the b quarks. We have chosen to use the correlation between the p_T of the highest p_T muon and the highest p_T b quark for this translation. For example, the muon threshold of 3 GeV/c corresponds to a b quark threshold of about 6 GeV/c, while the $p_{T\mu}$ range 7-10 GeV/c corresponds to $p_{Tb} \gtrsim 11$ GeV/c. Applying these cuts to the higher p_T quark of the $b\bar{b}$ pair (p_{Tb}^{high}), we then use the effective $O(\alpha_s^3)$ Monte Carlo to extrapolate to the cross-section for unlimited p_{Tb}^{low}, unlimited mass range ($m(b\bar{b}) > 2m_b$), and all rapidities.

These measured cross-sections are compared to the central predictions of the $O(\alpha_s^3)$ QCD calculation in fig. 6. The factors used to normalize these predictions to the data are all within the large theoretical uncertainties of about 40% for the last bin of the $\Delta\phi$ distribution, and about a factor 2 for the other bins and ΔR [12]. Good agreement is observed for both the $\Delta\phi$ and ΔR distributions. This topological agreement is a highly nontrivial test of the underlying QCD dynamics.

While the leading order $O(\alpha_s^2)$ contributions produce back-to-back configurations ($\Delta\phi = 180°$) and hence only populate the last bin of the $\Delta\phi$ distribution, higher order processes can yield any $\Delta\phi$ value.

For an approximate separation of the lowest and higher order contributions we therefore introduce the concept of *(quasi-)2-body* and *3-body* final states, which we *define* as

$$\begin{aligned} 2-body\ final\ state &\equiv \Delta\phi(b\bar{b}) > 150° \\ 3-body\ final\ state &\equiv \Delta\phi(b\bar{b}) < 150° \end{aligned} \tag{7}$$

An example for a 3-body event is shown in fig. 7. The many advantages of this phenomenological definition are discussed in detail in ref. [10].

Correcting for acceptance using the same procedure as for the single inclusive cross-section, we obtain the cross-sections for single b quark production originating from 2-body and 3-body final states quoted in table 7 and shown in fig. 8.

Good agreement with the differential QCD calculation of Mangano, Nason, and Ridolfi [9] is again observed for both shape and normalization. From the measured 3-body

Table 7: *Cross-sections for single b quark production with unrestricted rapidity range. Only the results for dimuons from different quarks are considered. The total cross-section is separated into cross-sections for 2-body and 3-body final states. Only the p_T-dependent errors are quoted. A common p_T-independent systematic error of 28% has to be added in quadrature (except for the 3-body fraction) to obtain the total errors.*

$p_T\mu_1$ [GeV/c]	$p_T^{min}(b)$ [GeV/c]	inclusive cross-section [μb]	2-body cross-section [μb]	3-body cross-section [μb]	3-body fraction [%]
3-5	6	3.20 ± 0.35	2.02 ± 0.46	1.18 ± 0.40	37 ± 11
5-7	8	1.69 ± 0.13	1.09 ± 0.13	0.60 ± 0.11	36 ± 6
7-10	11	0.463 ± 0.065	0.245 ± 0.041	0.218 ± 0.041	47 ± 6
10-20	15	0.108 ± 0.033	0.064 ± 0.018	0.044 ± 0.025	41 ± 22

fraction, the presence of higher order contributions is again established with a significance of more than seven standard deviations.

Since these semi-differential cross-sections and angular distributions are the first measurements of their kind for hadronically produced b quark pairs, a comparison with other experiments is not yet possible. On the other hand, from a comparison of the *single b* quark measurements of UA1 [1] and CDF [24], speculations about a possibly large contribution from non-perturbative gluon fragmentation into $b\bar{b}$ pairs [25] have been raised. Since (quasi-)collinear b quark emission is expected for such a contribution, it should show up in the data as a sizeable excess over the $O(\alpha_s^3)$ prediction in the low $\Delta\phi$ and ΔR range.

Assuming that the $b\bar{b}$ opening angle in space for such a contribution will be less than 90° for central rapidities (corresponding to $\Delta R < 1.6$), an upper limit can be derived from the data.

- The *measured* cross-sections for $\Delta R < 1.6$ can be directly obtained from the first two data points in the ΔR distribution, yielding

$$\sigma(\Delta R < 1.6,\ p_{Tb}^{high} > 6\ GeV/c) = \quad 0.38 \pm 0.21_{stat}\ \mu b \tag{8}$$

$$\sigma(\Delta R < 1.6,\ p_{Tb}^{high} > 11\ GeV/c) = \quad 0.084 \pm 0.044_{stat}\ \mu b \tag{9}$$

- The *expected* perturbative QCD cross-section can be extrapolated using the shape predicted by the $O(\alpha_s^3)$ calculation. Normalizing the prediction to the data excluding the $\Delta R < 1.6$ range, and extrapolating towards $\Delta R = 0$, the expected

cross-sections are

$$\sigma(\Delta R < 1.6,\ p_{Tb}^{high} > 6\ GeV/c) = \quad 0.42 \pm 0.13_{sys}\ \mu b \tag{10}$$

$$\sigma(\Delta R < 1.6,\ p_{Tb}^{high} > 11\ GeV/c) = \quad 0.090 \pm 0.027_{sys}\ \mu b \tag{11}$$

in excellent agreement with the measured numbers, where the error reflects the 30% uncertainty due to the variation of the theoretical shape.

- Subtraction of the expected cross-sections from the measured ones then yields upper limits for an *additional* contribution from nonperturbative gluon fragmentation into $b\bar{b}$ pairs

$$\sigma_{nonpert.}(\Delta R < 1.6,\ p_{Tb}^{high} > 6\ GeV/c) < \quad 0.37\ \mu b \quad @\ 90\%\ c.l. \tag{12}$$

$$\sigma_{nonpert.}(\Delta R < 1.6,\ p_{Tb}^{high} > 11\ GeV/c) < \quad 0.079\ \mu b \quad @\ 90\%\ c.l. \tag{13}$$

- Comparing this with the corresponding cross-sections for unlimited ΔR, the two limits can be combined into a single statement:

$$\sigma_{nonpert.}(\Delta R < 1.6)/\sigma_{all} < 11\% \quad @\ 90\%\ c.l. \tag{14}$$

in the measured range 6 GeV/$c \lesssim$ p$_{Tb}^{high} \lesssim$ 15 GeV/c and $|y| \lesssim 2$.

Since the QCD prediction of Mangano, Nason, and Ridolfi does not allow the calculation of angular distributions corresponding to specific $O(\alpha_s^3)$ matrix elements (and their interference terms) only, a measurement of the contribution from *perturbative* gluon fragmentation (quasi-collinear gluon splitting) based on this calculation is not possible. However, according to the fit of the ISAJET-predicted shapes to the data (fig. 5), 60 ± 34 % of the events contributing to the cross-section (11) originate from gluon splitting processes. From a rough comparison with the measured UA1 jet cross-sections [26], this result is consistent with the prediction [27] that in the E$_T$ range 20-30 GeV 1-2% of the gluon jets should fragment into a $b\bar{b}$ pair, typically yielding b quarks in the p$_T$ range 10-15 GeV/c.

9 Conclusions

Aiming at a measurement of $b\bar{b}$ correlations, we have made a detailed study of dimuon mass and angular distributions. All contributing processes are in good agreement with expectations. In particular, the contributions from heavy flavour events ($b\bar{b}$+$c\bar{c}$) can be reliably extracted.

The separation of the (small) charm contribution from the contributions from 1st and 2nd generation beauty decays yields simultaneous measurements of the cross-section for beauty production and of the $B^0\bar{B}^0$-mixing parameter. The obtained mixing parameter

$$\chi = 0.157 \pm 0.020_{stat} \pm 0.032_{sys} \tag{15}$$

is consistent with our earlier results [4, 5] and with similar measurements from other experiments [28].

The explicit and detailed consideration of the effect of $b\bar{b}$ correlations yields improved measurements of the inclusive beauty production cross-section from dimuon events, in excellent agreement with the $O(\alpha_s^3)$ QCD prediction of Nason, Dawson, and Ellis. Using the shape of this prediction to extrapolate to $p_T = 0$ and to all rapidities, an improved measurement of the total $b\bar{b}$ cross-section at the Sp$\bar{p}$S collider

$$\sigma_{tot}(p\bar{p} \rightarrow b\bar{b}X) = 19.7 \pm 4.3_{exp}\ ^{+10.4}_{-6.5}{}_{th}\ \mu b \tag{16}$$

is obtained.

The measured $b\bar{b}$ angular distributions are found to be in good agreement with the $O(\alpha_s^3)$ QCD predictions of Mangano, Nason, and Ridolfi, and can be phenomenologically reproduced by the ISAJET Monte Carlo within known limitations. From these distributions, we establish the predicted large contribution from higher order QCD processes (about 30-40% depending on the 'higher order' definition) with a significance of about seven standard deviations. A nonzero contribution to the cross-section from final state gluon splitting (involving the presence of an intermediate 3-gluon vertex) is obtained at 95% confidence level. The absence of an excess of events with small $b\bar{b}$ opening angles is used to place a limit on a contribution from nonperturbative gluon fragmentation into $b\bar{b}$ pairs

$$\sigma_{nonpert}(\Delta R(b\bar{b}) < 1.6)/\sigma_{all} < 11\% \ \ @\ 90\%\ c.l. \tag{17}$$

for a p_T of the larger p_T b quark in the range 6-15 GeV/c and $|y| < 2$. The contribution from perturbative gluon fragmentation is found to be consistent with expectations.

In general, the good agreement of the measured $b\bar{b}$ correlations with QCD predictions is interpreted as a successful test of the corresponding QCD matrix elements.

Acknowledgements

We are grateful to the authors of ref. [9] and in particular to P. Nason for providing us with the program for the $O(\alpha_s^3)$ QCD calculation and instructing us how to use it.

We are thankful to the management and staff of CERN and of all participating institutes for their vigorous support of the experiment. The following funding agencies have contributed to this program:

Fonds zur Förderung der Wissenschaftlichen Forschung, Austria.
Valtion luonnontieteellinen toimikunta, Suomen Akatemia, Finland.
Institut National de Physique Nucléaire et de Physique des Particules and Institut de Recherche Fondamentale (CEA), France.
Bundesministerium für Forschung und Technologie, Germany.
Istituto Nationale di Fisica Nucleare, Italy.
Science and Engineering Research Council, United Kingdom.
Stichting Voor Fundamenteel Onderzoek der Materie, The Netherlands.
Centro de Investigaciones Energetica, Medioambientales y Tecnologicas (CIEMAT), Spain.
Department of Energy, USA.

Thanks are also due to the following people who have worked with the collaboration in the preparations for and data collection on the runs described here: L. Baumard, F. Bernasconi, D. Brozzi, V. Cecconi, L. Dumps, G. Fetchenhauer, G. Gallay, S. Lazic, J.C. Michelon, S. Pavlon and L. Pollet.

References

[1] UA1 collaboration, C. Albajar et al., Phys. Lett. **B 256** (1991) 121

[2] UA1 collaboration, C. Albajar et al., *Drell-Yan and Upsilon production at the CERN $p\bar{p}$ collider*, to be published;
A. Moulin (UA1 collaboration), proceedings of the 21^{st} International Symposium on Multiparticle Dynamics, Wuhan, China, 23-27 september 1991 (World Scientific, Singapore, 1992) p. 221

[3] UA1 collaboration, C. Albajar et al., Phys. Lett. **B 213** (1988) 405

[4] UA1 collaboration, C. Albajar et al., Phys. Lett. **B 186** (1987) 247

[5] UA1 collaboration, C. Albajar et al., Phys. Lett. **B 262** (1991) 171

[6] UA1 collaboration, C. Albajar et al., Phys. Lett. **B 186** (1987) 237

[7] UA1 collaboration, C. Albajar et al., Z. Phys. **C 37** (1988) 489

[8] see e.g. :
N. Ellis and A. Kernan, Phys. Rept. **195** (1990) 23

[9] M.L. Mangano, P. Nason, and G. Ridolfi, Nucl. Phys. **B373** (1992) 295

[10] UA1 collaboration, C. Albajar et al., *Measurement of α_s from $b\bar{b}$ production at the CERN $p\bar{p}$ collider*, to be published;
A. Geiser (UA1 collaboration), proceedings of the XXVIIth Rencontre de Moriond, Perturbative QCD and Hadronic Interactions, Les Arcs, France, 22-28 march 1992, ed. by Tran Thanh Van (Editions Frontières, Gif-sur-Yvette,1992) p. 159

[11] UA1 collaboration, C. Albajar et al., Z. Phys. **C 48** (1990) 1, and references therein

[12] A. Geiser, Ph.D. thesis, RWTH Aachen 1992, Aachen report PITHA 92/31

[13] UA1 collaboration, C. Albajar et al., Phys. Lett. **B 209** (1988) 397

[14] UA1 collaboration, C. Albajar et al., Phys. Lett. **B 253** (1991) 503

[15] F. Paige and S.D. Protopopescu, *ISAJET Monte Carlo*, BNL 38034 (1986)

[16] D. Kuebel et al., ANL-HEP-PR-90-23 (1990)

[17] A. Moulin, Ph.D. thesis, RWTH Aachen 1993, Aachen report PITHA 92/24

[18] UA1 collaboration, C. Albajar et al., Phys. Lett. **B 256** (1991) 112

[19] UA1 collaboration, C. Albajar et al., Phys. Lett. **B 273** (1991) 540

[20] P. Nason, S. Dawson and R.K. Ellis, Nucl. Phys. **B303** (1988) 607;
P. Nason, S. Dawson, and R.K. Ellis, Nucl. Phys. **B327** (1989) 49

[21] T. Redelberger, Nucl. Phys. **B** (Proc. Suppl.) 1B (1988) 123

[22] G. Altarelli et al., Nucl. Phys. **B308** (1988) 724

[23] P. Nason, S. Dawson and R.K. Ellis, Nucl. Phys. **B303** (1988) 607

[24] CDF collaboration, F. Abe et al., Phys. Rev. Lett. **68** (1992) 3403;
CDF collaboration, F. Abe et al., Phys. Rev. Lett. **69** (1992) 3704;
CDF collaboration, F. Abe et al., FERMILAB-PUB-93/091-E (1993), submitted to Phys. Rev. Lett.;
CDF collaboration, F. Abe et al., FERMILAB-PUB-93/106-E (1993), submitted to Phys. Rev. Lett.;
CDF collaboration, F. Abe et al., FERMILAB-PUB-93/131-E (1993), submitted to Phys. Rev. **D**;
CDF collaboration, F. Abe et al., FERMILAB-PUB-93/145-E (1993), submitted to Phys. Rev. Lett.

[25] B. Lampe, INLO-PUB-12/91 (1991)

[26] UA1 collaboration, G. Arnison et al., Phys. Lett. **B 172** (1986) 461;
UA1 collaboration, C. Albajar et al., Nucl. Phys. **B309** (1988) 1

[27] M. Mangano and P. Nason, Phys. Lett. **B 285** (1992) 160

[28] MAC collaboration, H.R. Band et al., Phys. Lett. **B 200** (1988) 221;
Mark II collaboration, A.J. Weir et al., Phys. Lett. **B 240** (1990) 289;
L3 collaboration, B. Adeva et al., Phys. Lett. **B 252** (1990) 703;
ALEPH collaboration, D. Decamp et al., Phys. Lett. **B 258** (1991) 237;
CDF collaboration, F. Abe et al., Phys. Rev. Lett. **67** (1991) 3351;
OPAL collaboration, P.D. Acton et al., Phys. Lett. **B 276** (1992) 379;
ALEPH collaboration, D. Buskulic et al., Phys. Lett. **B 284** (1992) 177;
L3 collaboration, B. Adeva et al., Phys. Lett. **B 288** (1992) 395;
DELPHI collaboration, P. Abreu et al., Phys. Lett. **B 301** (1993) 145;
OPAL collaboration, R. Akers et al., CERN-PPE/93-106, submitted to Z. Phys. **C**

Figures

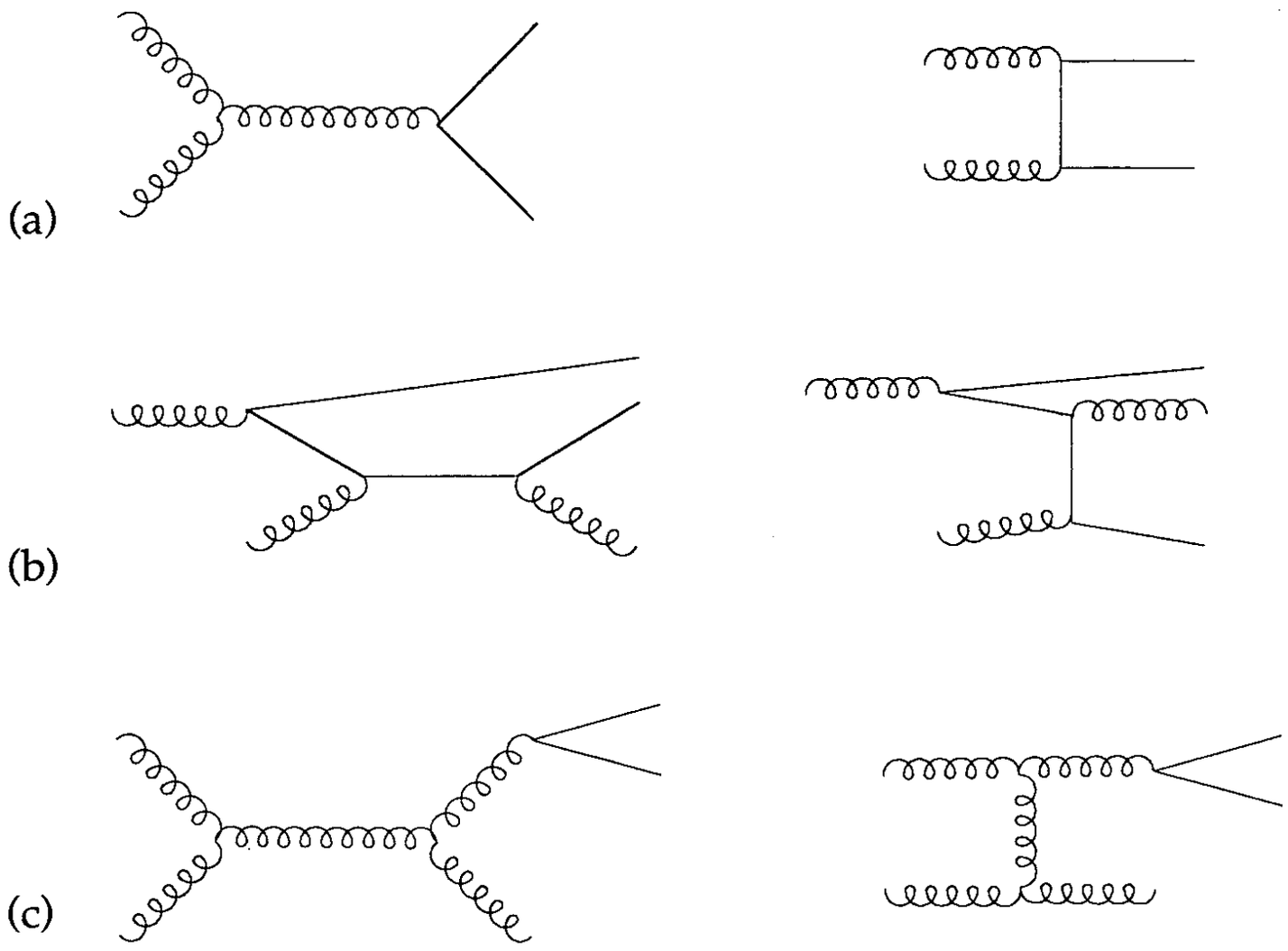

Figure 1: *Representative Feynman diagrams for heavy quark production by the processes of 'flavour creation' (a), initial state gluon splitting or 'flavour excitation' (b), and final state gluon splitting (c). Other possible processes include initial and final state gluon radiation from these diagrams, virtual diagrams, and interference effects.*

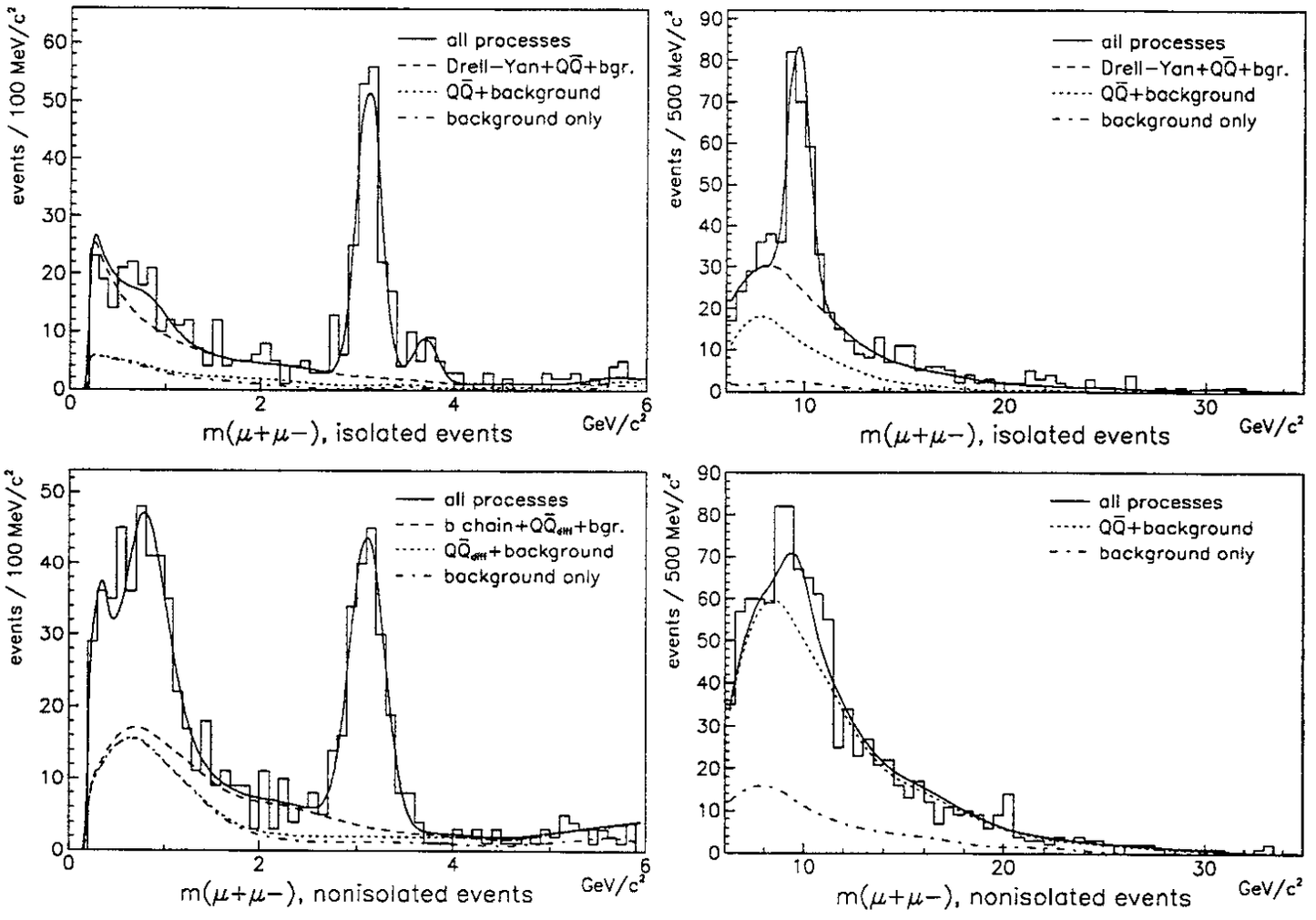

Figure 2: *Dimuon mass distributions for unlike sign muon pairs ($p_{T\mu} > 3$ GeV/c) as part of the overall mass and angle fit. The distributions for isolated (top) and nonisolated (bottom) events are shown separately for the mass ranges 0-6 and 6-35 GeV/c^2. The fit results are superimposed as curves. The curve 'all processes' includes contributions from Υ ($m = 9.5$ GeV/c^2), J/ψ ($m = 3.1$ GeV/c^2), $\psi\prime$ ($m = 3.7$ GeV/c^2), and low mass mesons (ρ, ω, ϕ, η and $\eta\prime$, $m \lesssim 1$ GeV/c^2), in addition to the Drell-Yan, heavy flavour ($Q\bar{Q} = b\bar{b}+c\bar{c}$), and background contributions, which are also shown separately. For the low mass nonisolated events, the heavy flavour contribution is shown separated into a (dominating) contribution from b chain decays, and a contribution of muon pairs originating from different heavy quarks ($Q\bar{Q}_{diff}$). The corresponding like sign distributions can be found in [12].*

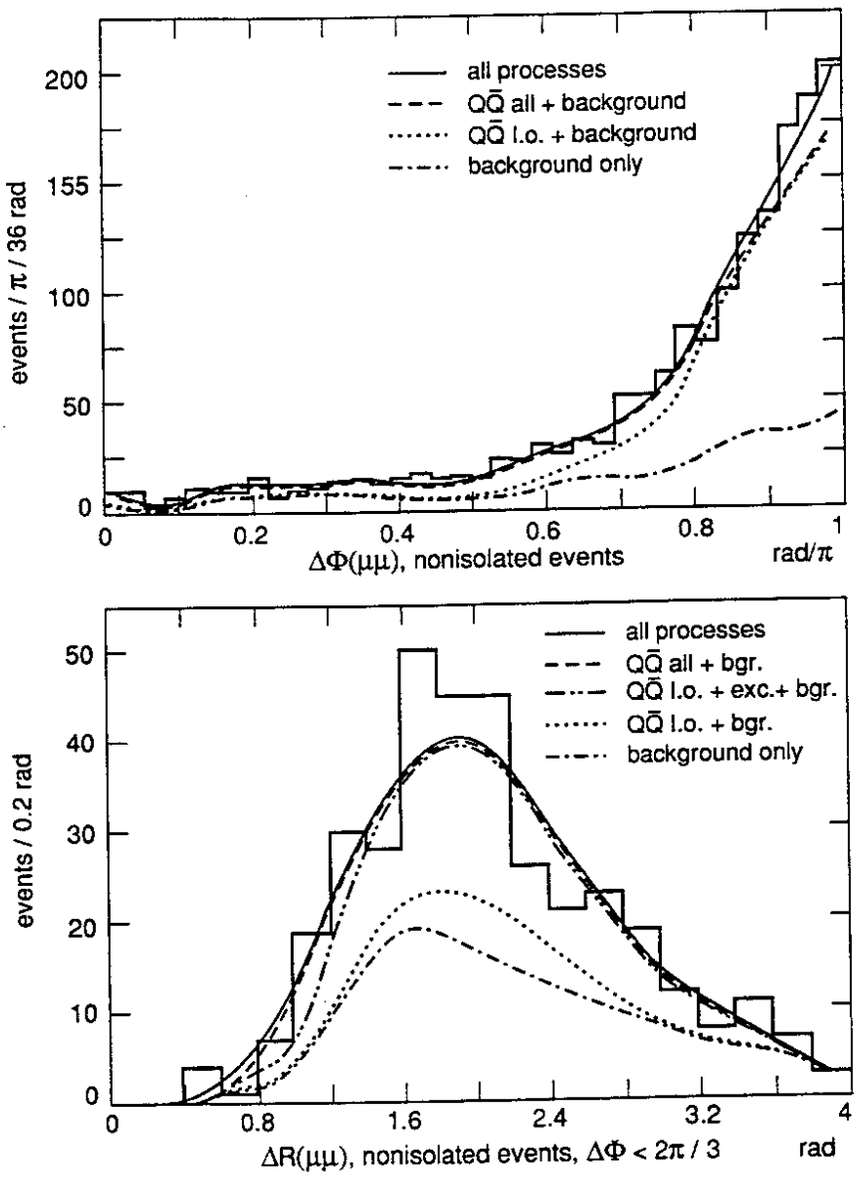

Figure 3: *Dimuon angular distributions for nonisolated muon pairs ($p_{T\mu} > 3$ GeV/c, $m_{\mu\mu} > 4$ GeV/c^2) as part of the overall mass and angle fit. Shown are the distributions for $\Delta\phi$ (azimuth angle) and ΔR ('space angle'). A cut of $\Delta\phi < 120°$ has been applied for the ΔR distribution. Also shown are the fit results for 'all processes' as listed in fig. 2, and for heavy flavour ($Q\bar{Q}$) production and background. The heavy flavour contribution is shown*
- for all subprocesses (flavour creation, also called 'ISAJET lowest order', flavour excitation, and gluon splitting),
- for all subprocesses except gluon splitting (l.o. + exc.), and
- for flavour creation only (l.o.).

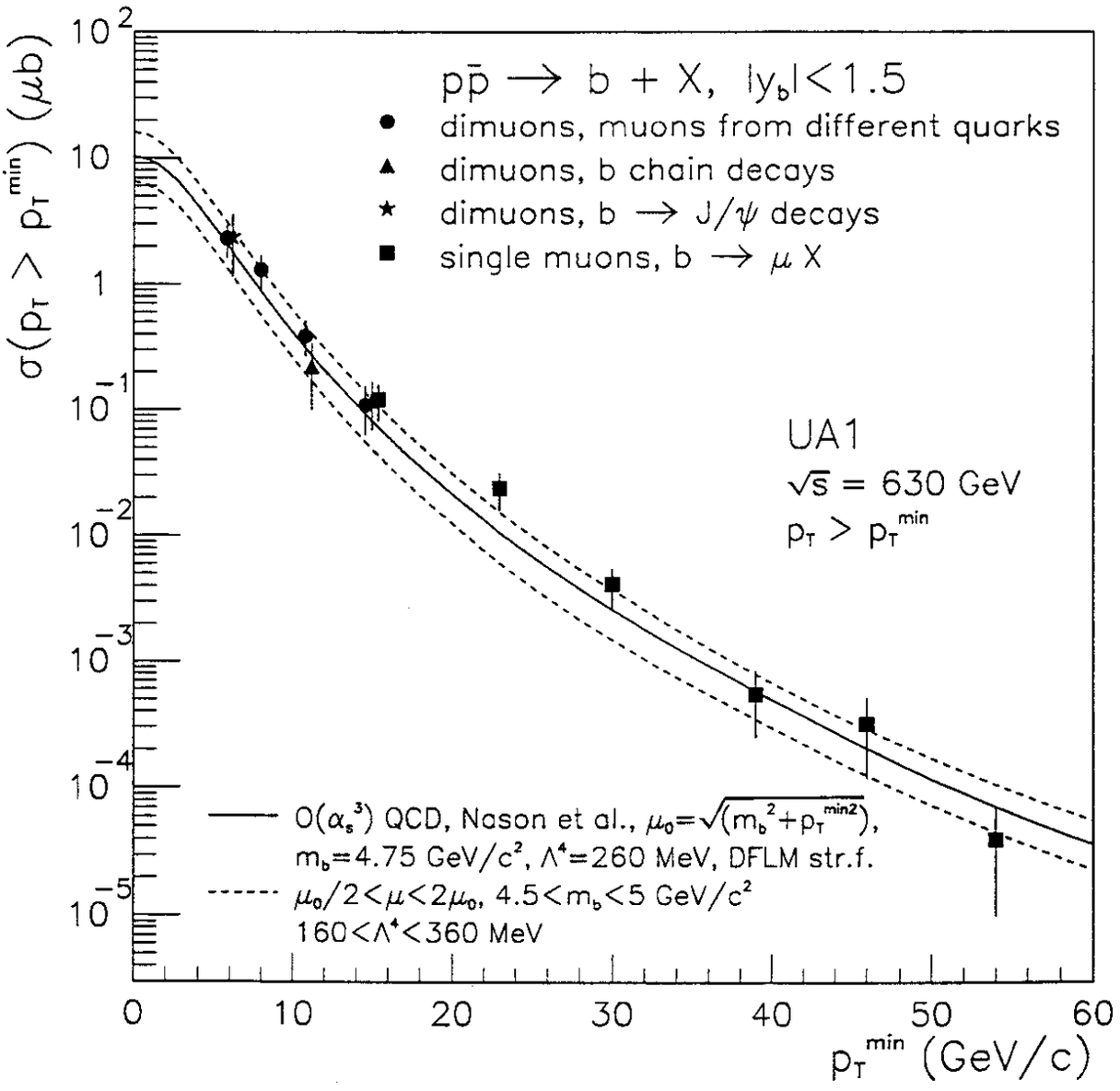

Figure 4: *The inclusive single b quark cross-section for $|y| < 1.5$ and $p_T > p_T^{min}$ in $p\bar{p}$ collisions at $\sqrt{s} = 630$ GeV. Also shown is the $O(\alpha_s^3)$ QCD prediction of Nason, Dawson, and Ellis [20].*

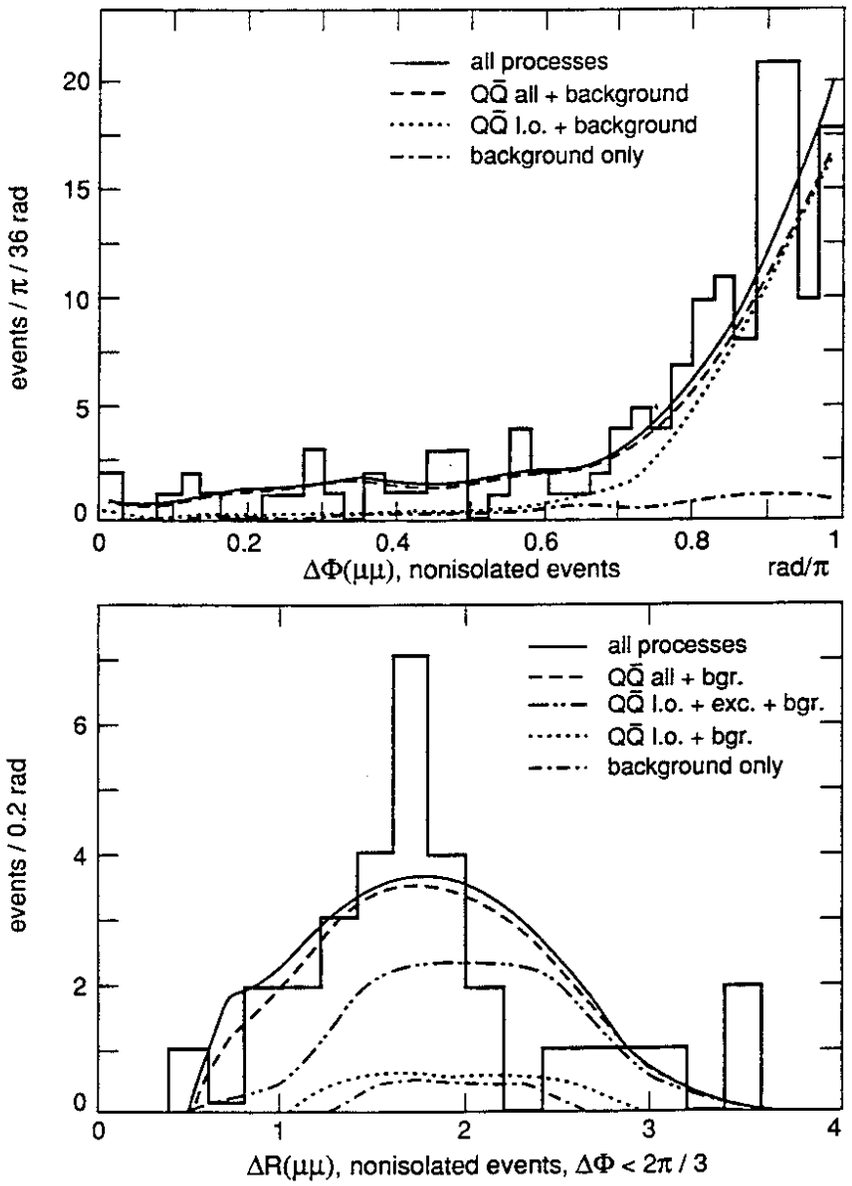

Figure 5: *Dimuon angular distributions for nonisolated muon pairs ($m_{\mu\mu} > 4$ GeV/c^2) as part of the overall mass and angle fit, for the p_T bin from 7-10 GeV/c. Shown are the distributions for $\Delta\phi$ (azimuth angle) and ΔR ('space angle'). A cut of $\Delta\phi < 120°$ has been applied for the ΔR distribution. Also shown are the fit results for 'all processes' as listed in fig. 2, and for heavy flavour ($Q\bar{Q}$) production and background. The heavy flavour contribution is shown*
- for all subprocesses (flavour creation, also called 'ISAJET lowest order', flavour excitation, and gluon splitting),
- for all subprocesses except gluon splitting (l.o. + exc.), and
- for flavour creation only (l.o.).

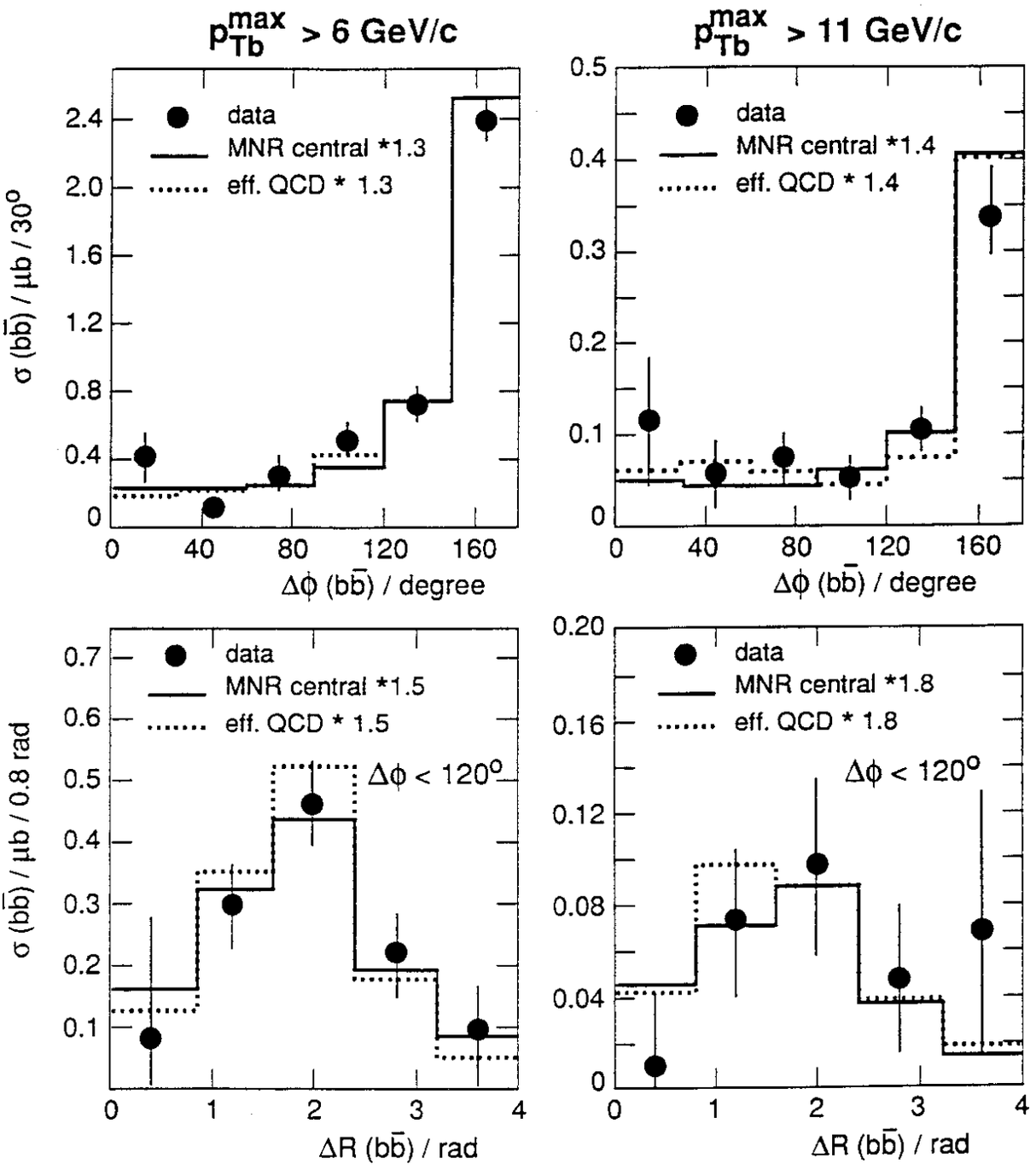

Figure 6: *Measured $b\bar{b}$ angular distributions for b quark pairs with a p_T of the higher p_T quark > 6 GeV/c (left) and > 11 GeV/c (right). Errors are statistical only. Shown are the distributions for $\Delta\phi$ (azimuth angle) and ΔR ('space angle'). A cut of $\Delta\phi < 120°$ has been applied for the ΔR distribution. Also shown are the central $O(\alpha_s^3)$ QCD predictions from the calculation of Mangano, Nason, and Ridolfi (MNR) [9] and the prediction of the effective QCD Monte Carlo [12] used for the acceptance calculation.*

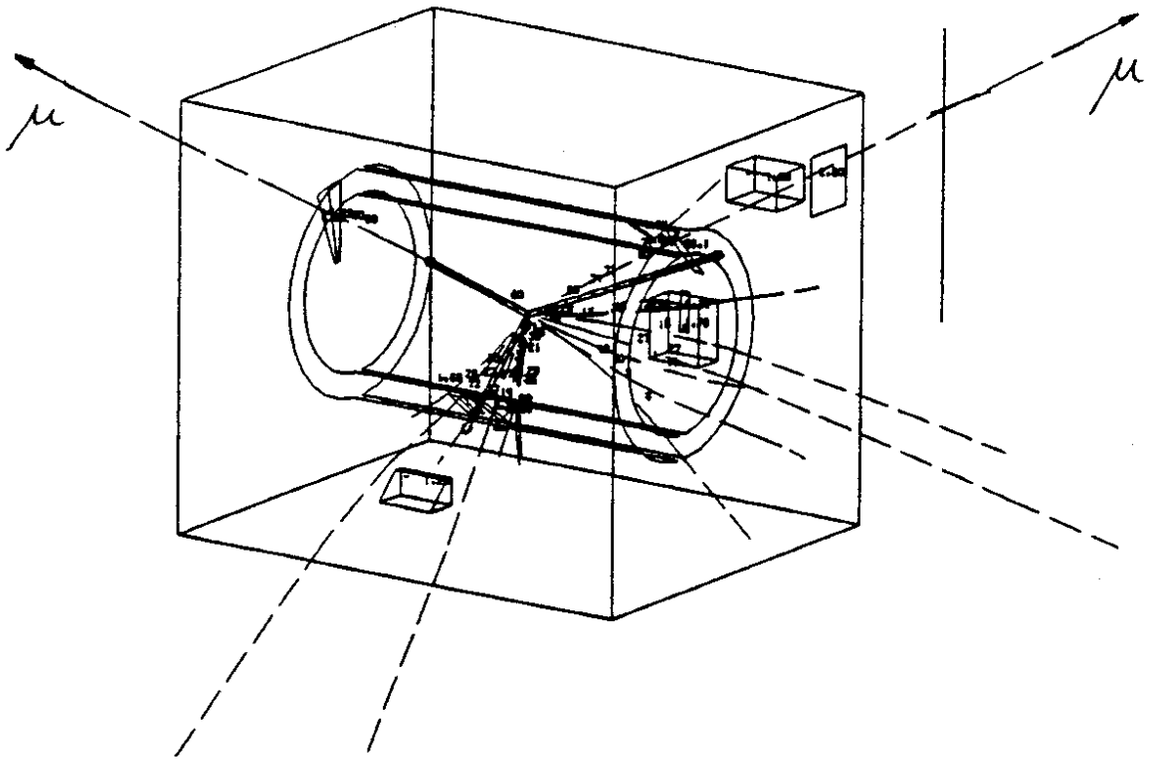

Figure 7: *Representation of a clear 3-body event. Only tracks with* $p_T > 1$ *GeV/c and calorimeter cells with* $E_T > 1$ *GeV are shown. The 3-body definition makes use of the muon directions only.*

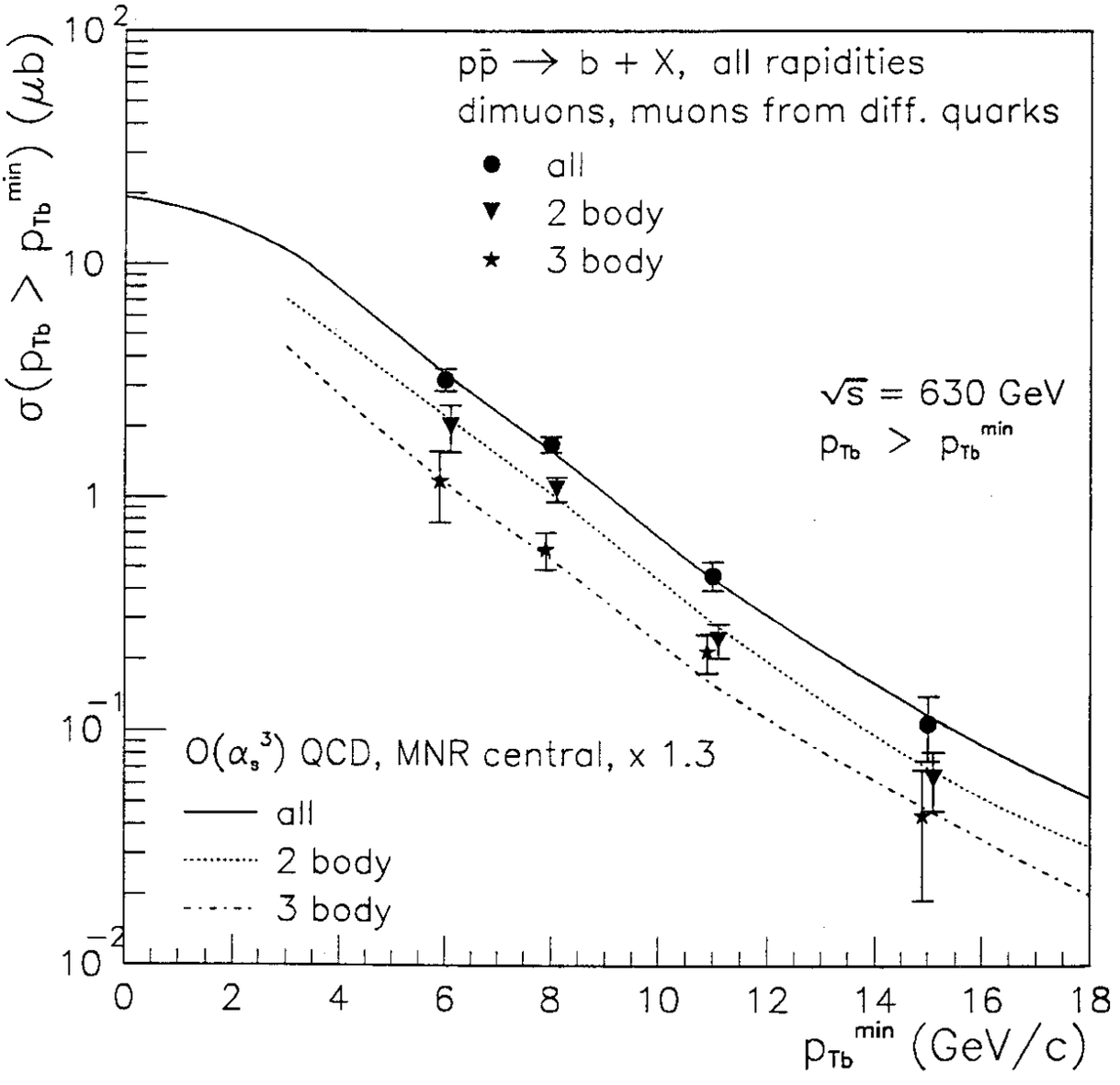

Figure 8: *The single b quark cross-section for all rapidities and $p_{Tb} > p_{Tb}^{min}$ in $p\bar{p}$ collisions at $\sqrt{s} = 630$ GeV. The inclusive cross-section is separated into cross-sections for b quarks from 2-body and 3-body final states. Only the p_T-dependent errors are shown. A global error of 28% has to be added to all data points. Also shown is the central prediction from the $O(\alpha_s^3)$ QCD calculation, normalized to the data using a global factor which is well within the theoretical error.*